

Crack Propagation Speed in the Drying Process of Paste

So KITSUNEZAKI*

Department of Physics, Graduate School of Human Culture, Nara Women's University, Nara 630-8506, Japan

We investigated crack propagation in the drying process of a thin layer of calcium carbonate ($CaCO_3$) paste experimentally. Cracks are induced by uniform desiccation from the top surface of a layer at the approximately same water content for various drying conditions. We found that the crack speed is a nonlinear increasing function of the drying rate at the cracking time although the tensile stresses arising in the bulk of paste do not depend practically on the drying rate. The crack speed does not depend significantly on the layer thickness and decreases in the cases in which glycerol is mixed to increase the viscosity of paste. These results suggest that dynamical crack growth occurs with viscoplastic relaxation in the vicinity of crack tips.

KEYWORDS: drying fracture, crack velocity, calcium carbonate paste, rheology, plastic deformation, relaxation process

1. Introduction

Cracks in pastes, such as clay and paint, are formed in a drying process in which the paste changes from a fluidlike state to a consolidated state with loss of fluid. The formation and variety of crack patterns in drying pastes have been investigated thoroughly.^{1–14)} A fracture process depends on both the porous and rheological properties of paste. For example, the columnar structure of cracks in starch pastes is formed with the propagation of a drying front, and the front is inferred to be caused by vapor and water transportation in paste.^{15–19)} Another example is the memory effect found by Nakahara et al. (called the Nakahara effect) recently. They reported that a preferential crack direction can be made in several types of pastes by shaking a layer of paste before drying.^{20–22)}

We investigate the growth processes of quasi-two-dimensional cracks induced by uniform desiccation from the open surface in a thin layer of paste. In this system, cracks are caused by stresses increasing gradually owing to the difference in contraction rate between the paste and the bottom of the container, and are created sequentially to form a typical mud-crack pattern with T-shape intersections in the middle stage of the drying process. The motion of a crack tip in such crack growth is sufficiently slow to observe with the naked eyes, and the failure cross sections exhibit distinctive patterns with fine stripes known as plumose structures, as shown in Fig. 1.^{23,24)} These features are different from those of the brittle failure of completely dried pastes, which allows rapid crack propagation to create approximately smooth fracture surfaces.

As per our knowledge, the growth speeds of cracks in drying pastes were measured for mixtures of water and coffee powder by Groisman and Kaplan,¹⁾ and for corn-

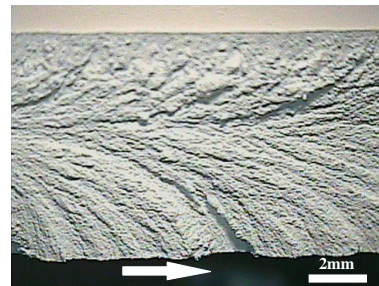


Fig. 1. Plumose structure on a fracture surface of $CaCO_3$ paste. This crack grew in the direction indicated by the arrow.

starch pastes by Müller and Dahm.²⁴⁾ Their measurements were carried out for several samples, and both experiments commonly indicated that the speed of a crack is approximately constant except near the boundaries, while it varies significantly among cracks. On the other hand, the measured values were considerably different between the two experiments. The speed ranges from 0.2 to 2 mm/min in the former and from 2 to 200 mm/s in the latter. This marked difference suggests that the crack speed depends significantly on the type of paste material.

In this paper, we report the measurements of crack speeds in a layer of $CaCO_3$ paste, which was dried at a constant temperature while monitoring the weight. One basic question on the crack growth in paste is about whether or not cracks propagate dynamically. In ordinary homogeneous materials, cracks are generally unstable once they start to grow with increases in uniform tensile stresses in the bulk, and they do not stop growing unless the stresses decrease. The cracks propagate rapidly to break the sample quickly in brittle solids, or propagate steadily to balance the release of elastic energy with the dissipation in viscoelastic materials, such

*E-mail: kitsune@ki-rin.phys.nara-wu.ac.jp

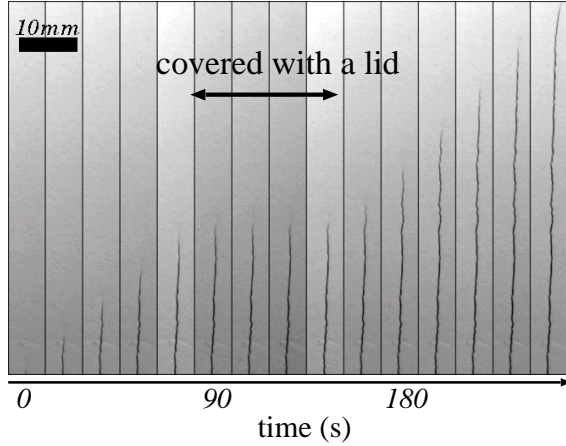


Fig. 2. Crack growing in a layer of $CaCO_3$ paste. It stopped propagating when desiccation was prevented by a lid. The series of photographs was taken at intervals of 18 s. The experimental setup was the same as that described in §2 and $m_{\text{last}} = 80.2$ g.

as gels. In contrast, we found that cracks in paste stop growing when desiccation is prevented and the crack tips remain at rest until drying starts again, as shown in Fig. 2, although the stresses at the cracking time do not depend on the drying rate. Thus, cracks in paste seem to grow quasistatically under the conditions in which the dynamical growth should be induced.

After describing the experimental methods and image processing, we report the dependencies of the crack speed on the drying rate and the layer thickness in §2. Here, we also investigate the effect of the viscosity of pore fluid by adding glycerol into paste. The measurements of the layer thickness and the stress acting on a lateral boundary of paste are reported in §3. We discuss the fracture mechanism of paste in §4. The summary of the experimental results and the conclusions are presented at the beginning of §4 and in §5, respectively.

2. Measurements of Crack Speeds

2.1 Experimental methods

We used fine powder of heavy calcium carbonate (*Nitto Funka Kogyo*, NS#600) to make pastes. Its true specific gravity, which is the mass divided by the volume of solid material excluding all pores, is $\rho_p = 2.7$ g/cm³ and the size of a grain is distributed from 0 to 10 μm around the average 1.5 μm . Unless otherwise noted, we mixed the powder with pure water using the mass ratio (water) : (powder) = 7 : 10 initially and poured the paste into a square acrylic container with sides of 120 mm, which was placed horizontally.

The crack speed varies significantly from one crack to the next in the same sample of paste, as observed in the preceding research studies.^{1,24} We could reduce such a variation significantly by the following procedures. The primary cause is inferred to be the differences in bound-

ary conditions between cracks, which depend on the place of the originating point and the previously formed cracks. Because bubbles left on the surface of paste can often be the origins of cracks, we first deaerated a well-churned paste in vacuum to remove fine bubbles and then poured it into the container after stirring it gently. Additionally, we utilized the Nakahara effect to make approximately straight and parallel cracks. We oscillated the paste horizontally for about 2 min at a frequency f_0 using a shaker (*Wakenyaku Model-2240*) before drying. The frequency was changed depending on the thickness of paste, h , as $f_0 \propto h^{-1/2}$ so that the shear stresses exerted at the bottom of paste would remain the same.²⁰

The pastes were dried in the apparatus depicted in Fig. 3. The air in the apparatus was dried continuously with a dehumidifier and convection was forced. The temperature over the sample was regulated at $40 \pm 1^\circ\text{C}$ using a heater and a controller (*Kenis Thermoeye ULE*). The temperature, humidity, and mass of paste, $m(t)$, were measured with a data logger and an electric balance (*AND EK-600H*) every 1 min. $m(t)$ decreased down to a constant value m_{last} with drying. The decrease rate of $m(t)$ was approximately constant for pastes of $CaCO_3$ and water, while it decreased with drying in the cases in which glycerol was mixed in paste because the ratio of glycerol in pore fluid increases with loss of water. Cracks were formed in the middle of the drying process, and such formation did not change the decrease rate.

For pastes of $CaCO_3$ and water, we assumed the volume of powder as $V_p \equiv m_{\text{last}}/\rho_p$ by ignoring the small amount of water left on the surface of grains and calculated the volume of water, $V_w(t) \equiv (m(t) - m_{\text{last}})/\rho_w$, and the volume fraction $v_f(t) \equiv V_w(t)/(V_w(t) + V_p)$, where ρ_w is the specific gravity of water at 40°C . For a given crack, we defined the drying rate r as the average decrease rate of v_f over the period of 40 min centered at the cracking time. In the cases in which glycerol was added, we defined v_f as the total volume fraction of water and glycerol, and calculated it by assuming that the ratio of glycerol to powder did not change with drying.

We controlled the drying rate r by changing the magnitude of air convection in the apparatus. To decrease r , we covered the container with a cellophane film or a vinyl chloride film in some experiments (the data are indicated by \bullet and \blacktriangle , respectively, in the figures explained below). r could be reduced to $1/10 - 1/50$ the values of the cases in which the container was open (\blacksquare). For an intermediate r , we switched off the dehumidifier (\square).

2.2 Image processing

The images of a layer of paste were taken from directly above with a digital camera (*Canon EOS20D*) using an interval timer. The image resolution is determined by the length corresponding to one pixel on these digital images, $L \simeq 0.083$ mm, which slightly differs among experiments. We investigated cracks formed in the square

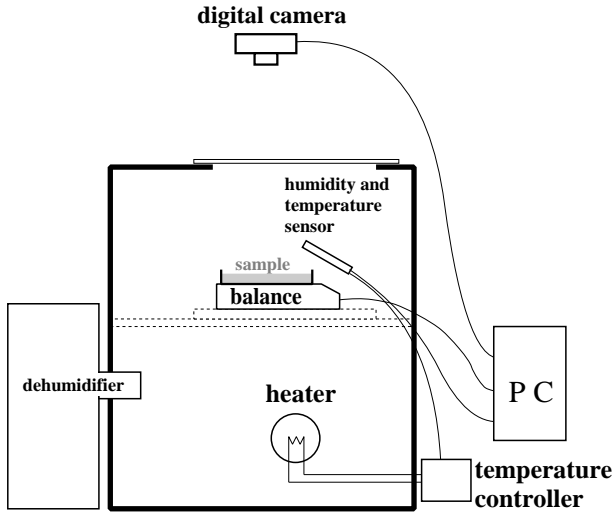


Fig. 3. Experimental setup.

center region with sides of 85 mm of the container and determined the crack speeds from the series of images using programs in accordance with the following procedures.²⁵⁾ (1) The skeleton of the crack pattern was extracted from an image by the Hilditch thinning algorithm after binary processing and denoising. The skeleton was disjointed into line segments corresponding to individual cracks by evaluating the connection at every vertex. (2) At each point on the skeleton, the cracking time was determined with a certain threshold from the increase in average brightness in the neighborhood of the radius $R = 10L$. Figure 4 shows an example of this analysis. (3) The crack speed at each point was determined by the least-squares method from the cracking times at an interval centered on the point, where the width of the interval was $600L$ measured along the crack. We analyzed cracks longer than 20 mm and used the data within a relative error of 2%. The definition of the length of a curve on digital images is not unique. The length of a crack is defined by $(A - \pi R^2)/2R$ from the area covered by the circular neighborhoods, A , in order to be insensitive to the fine jaggies of the crack and the thinning method.

2.3 Results

Cracks were first formed approximately perpendicular to the initial oscillation direction owing to the Nakahara effect after a few cracks appeared near the lateral walls of the container. The development of a crack pattern was different from that in directional drying experiments, where crack tips propagate all together with a drying front.^{2,6,10)} These cracks were created sequentially and their growth directions often varied even in the same sample. We observed that a few cracks sometimes grew simultaneously in opposite directions, especially for large drying rate, as shown in Fig. 5 (see the

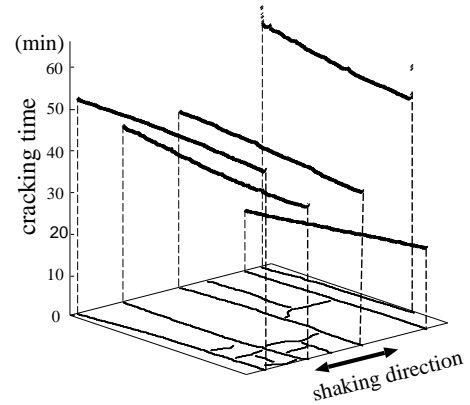


Fig. 4. Cracking times determined on the skeleton of a crack pattern. The pattern in the square region with sides of 85 mm is displayed at the bottom. The cracks were first formed parallel to one another because of the Nakahara effect.

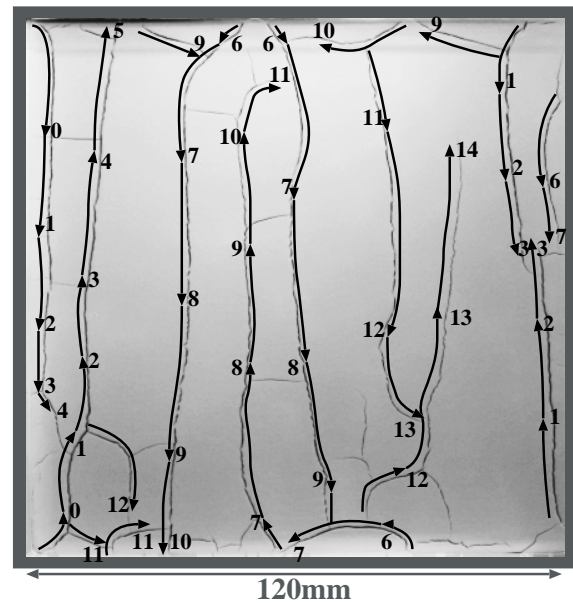


Fig. 5. Example of the development of a crack pattern. In this experiment, $m_{\text{last}} = 79.7 \text{ g}$ and $r = 1.46 \times 10^{-3} \text{ min}^{-1}$. We took photographs of the crack pattern at intervals of 8 s and checked every 10 images to trace the tips of main cracks. An arrow labeled with the number N indicates the position and growth direction of the crack tip at time $80N \text{ s}$.

arrows labeled with 8 for example).

As shown in Fig. 2, the crack speed essentially depends on the drying rate r at the cracking time, not on the history of drying. The crack speeds for various drying conditions are plotted with respect to the volume fraction v_f at the cracking time in Fig. 6(a). The decrease in v_f during the growth of each crack is small, which is the order of 10^{-3} for small r . The first crack in each experiment, indicated by a larger mark, is formed at

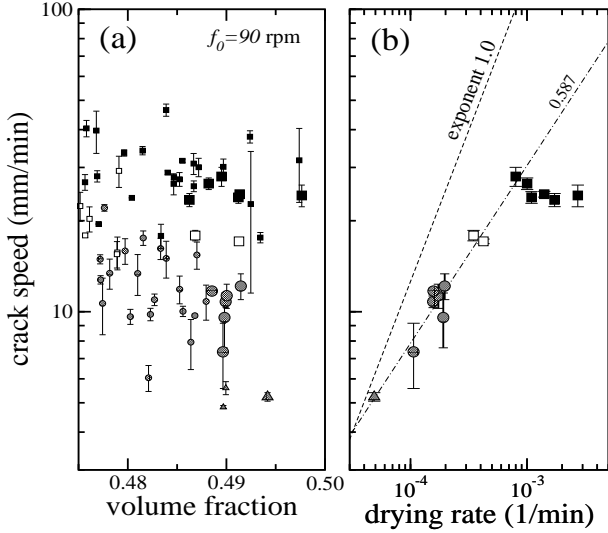


Fig. 6. (a) Dependence of the crack speed on the volume fraction v_f . (b) The speeds of the first cracks plotted with respect to the drying rate r on the double logarithmic scale. Each error bar indicates the change in speed during the crack growth. $m_{\text{last}} \approx 80$ g in all experiments.

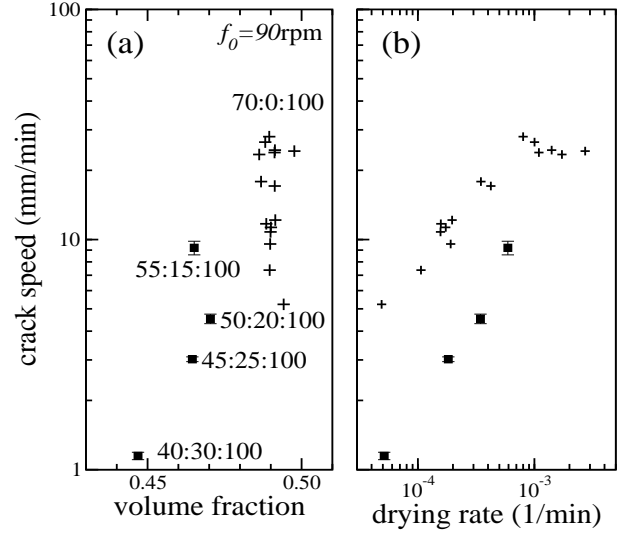


Fig. 8. The first-crack speeds in paste mixed with glycerol are plotted with respect to the (a) volume fraction v_f and (b) drying rate r . The initial mass ratios are indicated as (water) : (glycerol) : (powder). The data in Fig. 6(b) are indicated by ‘+’.

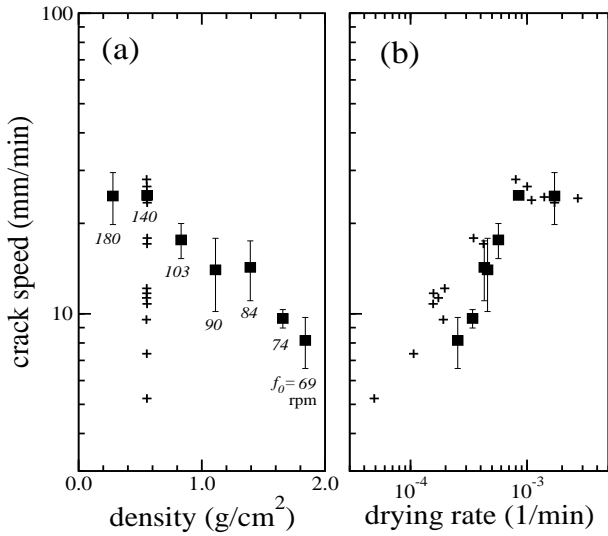


Fig. 7. (a) Dependence of the first-crack speed on the dry weight per unit area of the layer surface, which is proportional to the thickness h . (b) The same data are plotted with respect to r . The data in Fig. 6(b) are indicated by ‘+’ as reference.

$v_f = 0.48 - 0.50$ independent of r . The crack speed varies among subsequent cracks, while it tends to increase as v_f decreases. The data for the first cracks are plotted again with respect to r in Fig. 6(b). We find that the crack speed is an increasing nonlinear function of the drying rate and becomes approximately constant for large r . The exponent of this function is approximately 0.6 for $r < 10^{-3} \text{ min}^{-1}$.

The crack speed does not depend significantly on the thickness of paste. Figure 7 indicates the speeds of the first cracks for various thicknesses of paste, where the data in Fig. 6(b) are also plotted for comparison. The amount of water evaporated from the surface per unit time was almost the same for these experiments. Although the crack speed decreases as h increases in Fig. 7(a), we should note that r also changes inversely proportionally to h . Figure 7(b) indicates that this dependence is mainly due to the decrease in r .

The crack speed decreases as the viscosity of pore fluid increases. In the experiments for CaCO_3 paste mixed with glycerol, we prepared the same initial weight of paste for different ratios of glycerol to water. The pore fluid has large viscosity at the cracking time because the ratio of glycerol to water increases with drying. Figure 8(a) indicates the speeds of the first cracks with respect to the total volume fraction v_f of water and glycerol. v_f at the cracking time decreases slightly as the mass ratio of glycerol to powder increases, and no crack is formed when the mass ratio is larger than 0.3. The same data are plotted with respect to r in Fig. 8(b). From comparison at the same r , we find that the crack speed is significantly smaller than that in the cases in which glycerol is not mixed.

3. Measurements of Layer Thickness and Stress

In the drying process, paste first shrinks with a decrease in the amount of water, and then air penetrates into the paste to form liquid bridges among grains. To clarify the states of paste at the cracking time, we first investigated the change in layer thickness. We measured

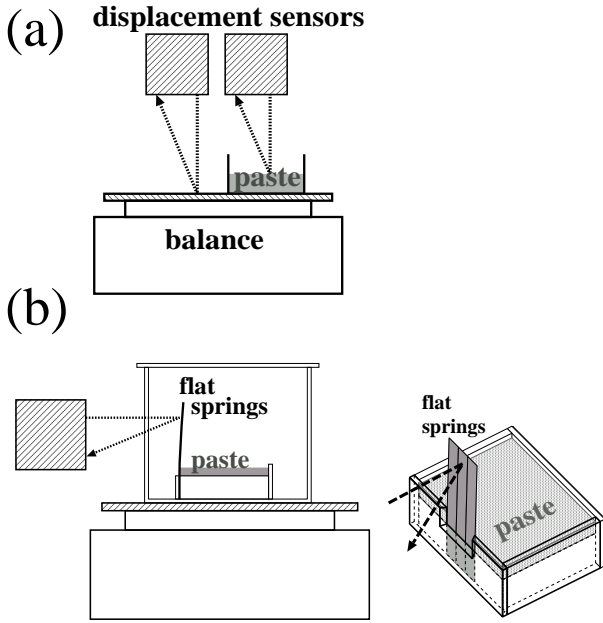


Fig. 9. Measurements of (a) thickness and (b) stress, where we used laser displacement sensors (*Sentec* CD1-30N). Paste was put in a teflon petri dish with a diameter of 50 mm in (a) and a square aluminum container with sides of 80 mm in (b). For (b), three springs with dimensions of $0.2 \times 8 \times 65 \text{ mm}^3$ (*Misumi* IBN) were fixed vertically on one side of the container so that they aligned with a slight gap, and we measured the displacement of the center one. The lateral walls except these springs were covered with teflon tape.

the thickness of a paste layer of CaCO_3 and water from the top using displacement sensors, and monitored the weight simultaneously, as depicted in Fig. 9(a). Figure 10 displays the results, where the abscissa denotes the volume ratio of water to powder, $V_w(t)/V_p$. We found that the thickness is determined by the amount of water and does not depend on the drying rate. It decreases linearly until cracking or detachment of paste from the lateral wall occurs, and then becomes approximately constant. This result indicates that air penetration does not begin practically at the cracking time and almost all the pores among grains are filled with water.

The stresses in the layer of paste increase with drying and are determined essentially by the volume fraction v_f . We investigated the stresses arising in a layer by measuring the horizontal displacement of a flat stainless-steel spring attached to the lateral boundary, as depicted in Fig. 9(b). Assuming that the paste pulled the spring horizontally and uniformly in the layer, we calculated the average stress from the displacement and the layer thickness estimated from the weight. Figure 11(a) shows that the average stress increases with drying until cracking. In this experiment, we prevented evaporation twice by putting a lid and confirmed that the increase in stress slowed down. We also carried out the measurements for

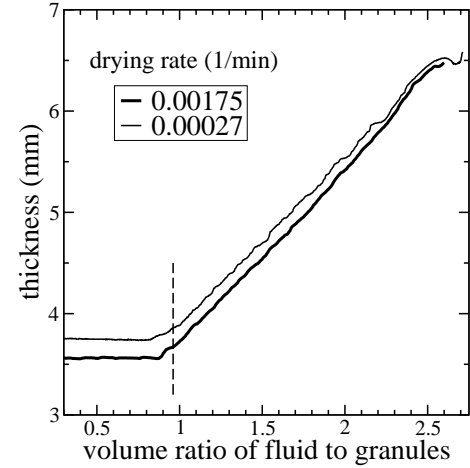


Fig. 10. Change in the thickness of paste. The numerical labels indicate the averages of drying rate in $0.48 < v_f < 0.50$. The initial pastes were approximately 20 g and the mass ratios were (water) : (powder) = 1 : 1 in these experiments. Cracking or detachment from the lateral wall occurred at the ratio indicated by the dotted line. Evaporation from the surface continued after that.

various drying conditions. In Fig. 11(b), the data in Fig. 11(a) and the data for a lower drying rate are plotted together with respect to v_f . We find that the stress does not depend on r .

These results indicate that pastes are in capillary states at the cracking time. In capillary states, negative pore pressure is caused in paste by the water-air interface on the free surface.^{26,27} The stress value at the cracking time in Fig. 11 is slightly below 100 kPa. It is on the same order as the hydrostatic pressure caused by a water-air interface with a curvature radius of a grain size, although we should regard this value as a rough estimate because the displacement of a spring is sensitive to the stress distribution.

The pore pressure p depends on the drying rate because a difference in pressure between the top and bottom of a layer is required to water fluxes caused by drying. However, we can justify that the difference is negligibly smaller than the stress at the cracking time. We carried out a falling head permeability test by assuming that the water fluxes obey Darcy's law $J = -(k/\mu)\nabla p$ in paste^{28,29} and obtained the permeability $k \simeq 4 \times 10^{-15} \text{ m}^2$ for saturated CaCO_3 pastes, where μ is the shear viscosity of water. The difference estimated from a typical drying rate is on the order of several 10 Pa at most.

4. Summary of the Results and Discussion

The main results of our experiments are summarized as follows. (R1) In a thin layer of CaCO_3 paste dried gradually from the free surface, cracks are created sequentially and their growth direction often varies. The

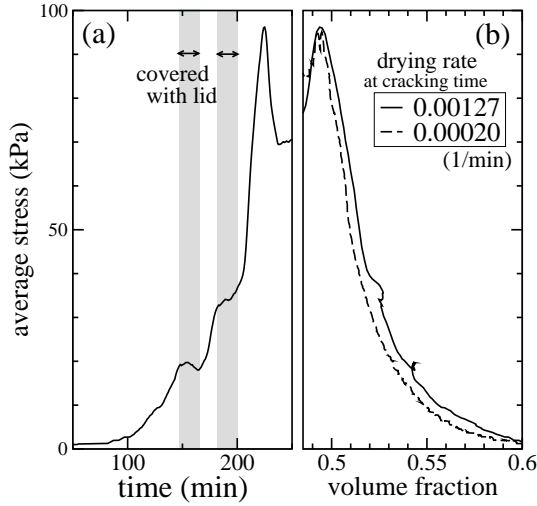


Fig. 11. Horizontal stress acting on the lateral boundary. The numerical labels indicate the average drying rates as in Fig. 10. The initial weights of paste were approximately 68 g.

crack formation does not change the drying rate r . (R2) The first crack is created at the approximately same volume fraction, $v_f = 0.48 - 0.50$, independent of r . (R3) At the cracking time, pastes are in capillary states and the stresses arising in the bulk of paste do not depend on r . (R4) Cracks grow at the speed depending on r at the time. They stop growing when drying is prevented. (R5) The crack speed is a nonlinear increasing function of r and does not depend significantly on the thickness of paste. (R6) The crack speed decreases when glycerol is mixed in paste.

4.1 States of paste at the cracking time

(R1)-(R3) indicate that paste is dried uniformly, and that the states are determined by v_f independently of the drying rate. These mean that the mechanical properties of paste at the cracking time do not also depend on the drying rate.

(R3) also indicates that the granular structure of paste is gradually compressed by drying because the counteracting forces of the negative pore pressure act on the free surface of paste in capillary states, as depicted in Fig. 12. Under such compressive states, we can assume that paste has a yield stress, below which it behaves elastically. Many experiments in soil mechanics have confirmed that the mechanical response of a saturated paste is determined by the effective stresses, which are defined as the differences between total stresses and pore pressure. Pastes are generally elastoplastic under compressive effective stresses and behave elastically until the anisotropy of stresses increases beyond a certain critical value.³⁰⁻³² It is also confirmed that the yield stress of $CaCO_3$ paste increases as v_f decreases,²⁰ although the mechanical characteristics of the paste have

not been investigated thoroughly as far as the author knows.

The effective stresses also act on the free boundaries created by a crack to open the crack further. In a conventional approach for mud crack patterns, a layer of paste are regarded as a network of linear springs and the system becomes subject to tensile stresses as the natural lengths decrease.⁷ Assuming that the paste is a linear elastic material except in the close vicinities of crack tips, the effective stresses acting on the surface of paste induce essentially the same stress concentration as supposed in the conventional approach because the compressive states are given by the superposition of a uniform stress to such tensile states.

From this discussion, we assume that (A1) paste at the cracking time is uniform and has mechanical properties independent of the drying rate, and (A2) paste behaves as an elastic material far from the crack tips. Next we apply the standard energetics of the fracture mechanics to the problem of crack growth in paste. For the energetics, we need to assume that the nonelastic regions in (A2) are localized in the close vicinities of the crack tips, although we should notice that it is not verified for cracking in paste. To confirm these assumptions, it is necessary to investigate the water and stress distributions in paste.

4.2 Crack growth depending on the drying rate

(R4) and (R5) raise a key question, that is, what mechanism can be responsible for such slow crack growth and the drying rate dependence of crack speed? The major differences of pastes from normal solids are their rheological and porous properties. A slow viscoplastic deformation is induced easily because of small yield stresses, and pore fluid can flow in paste. Considering these properties, we discuss two possible cases: (C1) paste exhibits a slow viscoplastic relaxation as a response to the stress concentration in the vicinities of crack tips, and (C2) water fluxes induce an interaction with a longer range than the layer thickness.

To clarify the following discussion, let us consider a simpler configuration in which a straight crack of length x grows in a 2-dimensional system with a fixed width $2H$, as depicted in Fig. 13. In our experiments, a paste layer hardly deforms at distances larger than the thickness from cracks due to the bottom boundary condition. Therefore, this system can be regarded as the primary deformable region surrounding a crack in the actual configurations by assuming H to be on the order of the layer thickness. We assume $x \gg H$ to focus on a sufficiently long crack compared with the thickness. The free energy of this system is generally written as

$$F = F_e(x; v_f) + G_0(v_f)x, \quad (1)$$

where F_e is the elastic energy and G_0 is the crack surface energy per unit length. The energy release rate

$G \equiv -\partial F_e/\partial x$ determines the stress concentration in the vicinity of the crack tip, which is a function of the effective stress σ and increases with drying. F dissipates with the crack growth. The energy dissipation for the crack growth of unit length,

$$-\frac{\partial F}{\partial x} = D_0(\dot{x}; v_f, \{G\}), \quad (2)$$

is determined by the viscoplastic response of paste to the stress concentration. Therefore, D_0 generally depends on x only through G implicitly, while it is an increasing function of \dot{x} due to the viscosity of paste.

The crack growth obeys eqs. (1) and (2). The drying rate $r = -\dot{v}_f$ is not included explicitly in these equations because of (A1). Substituting eq. (1), eq. (2) is rewritten as

$$D(\dot{x}; v_f, \{G\}) = G(x; v_f) - G_s(v_f, \{G\}) \geq 0, \quad (3)$$

where $D \equiv D_0(\dot{x}; v_f, \{G\}) - D_0(0; v_f, \{G\})$ and $G_s \equiv G_0(v_f, \{G\}) + D_0(0; v_f, \{G\})$. G_s is the minimum energy required to create a unit length of crack, which includes dissipation energy due to plastic deformation for mechanically quasistatic growth. The crack starts growing under the condition $G \geq G_s$. If $G - G_s$ decreases as x increases, the crack growth is quasistatic because $G = G_s$ gives a stable solution; otherwise, the crack propagates dynamically at the speed determined from eq. (3).³³⁾

The mechanism of crack growth in normal viscoelastic materials, such as gels, is not consistent with (R4) and (R5). If paste behaves elastically except in the vicinity of the crack tip, G does not depend on x for $x \gg H$; $G(x; v_f) \equiv G(v_f)$. In addition, if the response to stress concentration is so fast that D and G_s are determined from $G(v_f)$ at the time, the crack grows dynamically at the speed $\dot{x} = D^{-1}(G - G_s; v_f, G)$. This mechanism allows a slow crack growth for a large viscous dissipation, but not the drying rate dependence because \dot{x} is determined only from v_f .

Considering (C1), where D and G_s depend on the history of $G(v_f)$, we find a possibility for the drying rate dependence. Let us assume that the viscoplastic response is slow and G_s obeys the simplest relaxation rule with a single relaxation time τ ,

$$\tau \dot{G}_s = G - G_s. \quad (4)$$

If G increases slowly compared with τ as v_f decreases, $G_s \simeq G - \tau \dot{G}$ and then we obtain

$$\dot{x} = D^{-1}(G - G_s; v_f, \{G\}) = D^{-1}\left(\tau \frac{\partial G}{\partial v_f} \dot{v}_f; v_f, \{G\}\right). \quad (5)$$

Thus, the slow viscoplastic response of paste allows dynamic crack growth to depend on the drying rate. This mechanism is consistent, not only with (R4) and (R5), but also with (R6) because glycerol increases viscous dissipation to slow down the growth.

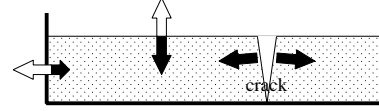


Fig. 12. Schematic picture of a cross section of a paste layer in a capillary state. White and black arrows denote pore pressures and effective stresses, respectively.

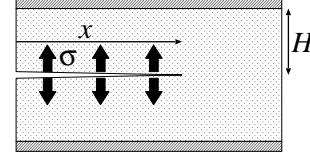


Fig. 13. Straight crack of length x . Its free surface is subjected to a uniform effective stress σ , and deformation is allowed in the 2-dimensional region of finite width $2H$.

On the other hand, in (C2), water transportation can induce an additional interaction in paste besides the elastic one. Therefore, the quasistatic crack growth is possible if $G(x; v_f) - G_s(v_f, G)$ decreases with x owing to this interaction. In this case, the crack grows with drying according to the solution of $G = G_s$, $x = g(v_f)$, and the crack speed is proportional to the drying rate as $\dot{x} = g'(v_f)\dot{v}_f$. However, this simple expectation of crack speed is not consistent with the nonlinear dependence in (R5).

Thus, our experimental results support dynamic crack growth with a slow viscoplastic response rather than quasistatic growth. It is a future problem to clarify the relaxation process concretely because we propose eq. (4) from simple mathematical consideration. Actual processes are more complex, and the viscoplastic response of paste may be affected by water transportation.

5. Conclusions

We investigated quasi-2-dimensional cracks formed with drying in a layer of $CaCO_3$ paste and found that the crack speed is a nonlinear increasing function of the drying rate. The speed is insensitive to the layer thickness and decreases as glycerol is mixed in paste. The cracks are created in capillary states and the stresses arising in the bulk of paste at the cracking time do not depend on the drying rate. These results suggest that plastic relaxation processes occur to prevent cracking in the vicinities of crack tips.

Acknowledgment

The author acknowledges A. Nakahara for some valuable advices on the experimental methods and T. Mizuguchi, A. Nishimoto, and C. Urabe for fruitful discussions. The author also thanks M. Aoki, a member

of our laboratory, for assistance with the experiments. This work is supported by JSPS through a Grant-in-Aid for Young Scientists B (KAKENHI 19740240).

- 1) A. Groisman and E. Kaplan: *Europhys. Lett.* **25** (1994) 415.
- 2) C. Allain and L. Limat: *Phys. Rev. Lett.* **74** (1995) 2981.
- 3) T. Hornig, I. M. Sokolov, and A. Blumen: *Phys. Rev. E* **54** (1996) 4293.
- 4) U. A. Handge, I. M. Sokolov, and A. Blumen: *Europhys. Lett.* **40** (1997) 275.
- 5) H. Ito and Y. Miyata: *J. Geol. Soc. Jpn* **104** (1998) 90 [in Japanese].
- 6) T. Boeck, H. -A. Bahr, S. Lampenscherf, and U. Bahr: *Phys. Rev. E* **59** (1999) 1408.
- 7) S. Kitsunozaki: *Phys. Rev. E* **60** (1999) 6449.
- 8) K. A. Shorlin, J. R. de Bruyn, M. Graham, and S. W. Morris: *Phys. Rev. E* **61** (2000) 6950.
- 9) K. -T. Leung and Z. Néda: *Phys. Rev. Lett.* **85** (2000) 662.
- 10) L. Pauchard, M. Adda-Bedia, C. Allain, and Y. Couder: *Phys. Rev. E* **67** (2003) 027103.
- 11) E. A. Jagla: *Phys. Rev. E* **69** (2004) 056212.
- 12) S. Bohn, L. Pauchard, and Y. Couder: *Phys. Rev. E* **71** (2005) 046214; S. Bohn, J. Platkiewicz, B. Andreotti, M. Adda-Bedia, and Y. Couder: *Phys. Rev. E* **71** (2005) 046215.
- 13) H. -J. Vogel, H. Hoffmann, and K. Roth: *Geoderma* **125** (2005) 203; H. -J. Vogel, H. Hoffmann, A. Leopold, and K. Roth: *Geoderma* **125** (2005) 213.
- 14) D. Mal, S. Sinha, T. R. Middya, and S. Tarafdar: *Physica A* **384** (2007) 182; D. Mal, S. Sinha, T. Dutta, S. Mitra, and S. Tarafdar: *J. Phys. Soc. Jpn.* **76** (2007) 014801.
- 15) G. Müller: *J. Geophys. Res.* **103** (1998) 15239.
- 16) A. Toramaru and T. Matsumoto: *J. Geophys. Res.* **109** (2004) B02205.
- 17) T. Mizuguchi, A. Nishimoto, S. Kitsunozaki, Y. Yamazaki, and I. Aoki: *Phys. Rev. E* **71** (2005) 056122.
- 18) L. Goehring, S. W. Morris, and Z. Lin: *Phys. Rev. E* **74** (2006) 036115.
- 19) A. Nishimoto, T. Mizuguchi, and S. Kitsunozaki: *Phys. Rev. E* **76** (2007) 016102.
- 20) A. Nakahara and Y. Matsuo: *J. Phys. Soc. Jpn.* **74** (2005) 1362; *Phys. Rev. E* **74** (2006) 045102(R); *J. Stat. Mech.* (2006) P07016.
- 21) M. Otsuki: *Phys. Rev. E* **72** (2005) 046115.
- 22) T. Ooshida: *Phys. Rev. E* **77** (2008) 061501.
- 23) R. Weinberger: *J. Struct. Geol.* **21** (1999) 379; *Geol. Soc. Am. Bull.* **113** (2001) 20.
- 24) G. Müller and T. Dahm: *J. Geophys. Res.* **105** (2000) 723; G. Müller: *J. Struct. Geol.* **23** (2001) 45.
- 25) We used ImageJ, which is a public domain image processing program (<http://rsbweb.nih.gov/ij>), and wrote plugins for the thinning processing and measurements.
- 26) S. Herminghaus: *Adv. Phys.* **54** (2005) 221.
- 27) N. Mitarai and F. Nori: *Adv. Phys.* **55** (2006) 1.
- 28) G. S. Campbell: *Soil Physics with BASIC -Transport Models for Soil-Plant Systems-* (Elsevier, Amsterdam, 1985).
- 29) W. A. Jury and R. Horton: *Soil Physics* (John Wiley & Sons, Hoboken, 2004) 6th ed.
- 30) D. M. Wood: *Soil Behaviour and Critical State Soil Mechanics* (Cambridge Univ. Press, New York, 1990).
- 31) P. Coussot: *Rheometry of Pastes, Suspensions, and Granular Materials* (John Wiley & Sons, Hoboken, 2005).
- 32) P. D. Hallett and T. A. Newson: *Eur. J. Soil Sci.* **56** (2005) 31.
- 33) B. N. J. Persson and E. A. Brener: *Phys. Rev. E* **71** (2005) 036123.